Composite UHDRS correlates with progression of imaging biomarkers in Huntington's disease

Estevez-Fraga, C.; Scahill, R.I.; Durr, A.; Leavitt, B.R.; Roos, R.A.C.; Langbehn, D.R.; ... ; Tabrizi, S.J.

Composite UHDRS Correlates With Progression of Imaging Biomarkers in Huntington's Disease

Carlos Estevez-Fraga, MD,[1] Rachael I. Scahill, PhD,[1] Alexandra Durr, MD, PhD,[2] Blair R. Leavitt, BSc, MDCM, FRCPC,[3] Raymund A.C. Roos, MD, PhD,[4] Douglas R. Langbehn, MD, PhD,[5] Geraint Rees, MD, PhD,[6] Sarah Gregory, PhD,[1] and Sarah J. Tabrizi, MD, PhD[1]*

[1]*Huntington's Disease Centre, Department of Neurodegenerative Disease, UCL Queen Square Institute of Neurology, London, UK* [2]*Sorbonne Université, Paris Brain Institute (ICM), AP-HP, Inserm, CNRS, Pitié-Salpêtrière University Hospital, Paris, France* [3]*Centre for Molecular Medicine and Therapeutics, Department of Medical Genetics, University of British Columbia, Vancouver, British Columbia, Canada* [4]*Department of Neurology, Leiden University Medical Center, Leiden, The Netherlands* [5]*Department of Psychiatry, University of Iowa, Iowa City, Iowa, USA* [6]*Wellcome Centre for Neuroimaging, UCL Queen Square Institute of Neurology, University College London, London, United Kingdom*

ABSTRACT: Background: The composite Unified Huntington's Disease Rating Scale (cUHDRS) is a multidimensional measure of progression in Huntington's disease (HD) being used as a primary outcome in clinical trials investigating potentially disease-modifying huntingtin-lowering therapies.
Objective: Evaluating volumetric and structural connectivity correlates of the cUHDRS.
Methods: One hundred and nineteen premanifest and 119 early-HD participants were included. Gray and white matter (WM) volumes were correlated with cUHDRS cross-sectionally and longitudinally using voxel-based morphometry. Correlations between baseline fractional anisotropy (FA); mean, radial, and axial diffusivity; and baseline cUHDRS were examined using tract-based spatial statistics.
Results: Worse performance in the cUHDRS over time correlated with longitudinal volume decreases in the occipito-parietal cortex and centrum semiovale, whereas lower baseline scores correlated with decreased volume in the basal ganglia and surrounding WM. Lower cUHDRS scores were also associated with reduced FA and increased diffusivity at baseline.
Conclusion: The cUHDRS correlates with imaging biomarkers and tracks atrophy progression in HD supporting its biological relevance. © 2021 International Parkinson and Movement Disorder Society

Key Words: Huntington's disease; composite Unified Huntington's Disease Rating Scale; diffusion tensor imaging; voxel-based morphometry; clinical trials; longitudinal

Huntington's disease (HD) is an autosomal-dominant neurodegenerative disorder, characterized by a slow progression of cognitive, psychiatric, and motor dysfunction.[1] Although the surge in HD clinical trials dictates the need for measures that can track disease evolution over short periods of time, clinical scales in HD show low reliability and validity[2-5] and investigate only isolated domains (ie, cognitive, motor) instead of the multiple aspects affected by the disease.

The composite Unified Huntington's Disease Rating Scale (cUHDRS) is a novel, multidomain measure encompassing motor, functional, and cognitive scales,[6] all of which are independently associated with HD severity.[7-9] The cUHDRS was generated to provide an improved measure of clinical progression using data from over 1600 early-HD patients. To form the composite, a signal-to-noise ratio (SNR) of different scales available as a part of the standard UHDRS[4] and also non-UHDRS rating scales[6] was performed dividing the change from baseline in a given measure by its standard deviation, followed by a principal component analysis of scales with the highest SNR. The cUHDRS has shown outstanding test–retest reliability, superior to its individual components, in terms of sensitivity to disease stage and longitudinally providing greater statistical power to detect clinical benefit.[6] As such, it is currently being used as a primary outcome measure in a huntingtin (HTT) lowering phase 3 clinical trial.[10]

Schobel et al demonstrated greater correlations between cUHDRS and global brain volumes relative to its subscales,[6] which is significant for therapies that limit neuronal loss. However, this work did not examine the relationship between cUHDRS and localized

***Correspondence to:** Dr. Sarah J. Tabrizi, Huntington's Disease Centre, UCL Queen Square Institute of Neurology, 2nd Floor Russell Square House, 10-12 Russell Square, WC1B 5EH London, United Kingdom, E-mail: s.tabrizi@ucl.ac.uk

†S.G. and S.J.T. are joint senior authors.

Relevant conflicts of interest/financial disclosures: S.J.T. was the global principal investigator (PI) for TRACK-HD. A.D., B.R.L., and R.A.C.R. were site PIs for Paris, Vancouver, and Leiden respectively. No other relevant disclosures or conflicts of interest.

Funding agencies: S.J.T. is partly supported by the UK Dementia Research Institute that receives its funding from DRI Ltd., funded by the UK Medical Research Council, Alzheimer's Society, and Alzheimer's Research UK. C.E.-F., S.G., R.I.S., G.R., and S.J.T. receive support from a Wellcome Trust Collaborative Award (200181/Z/15/Z).

Received: 14 May 2020; **Revised:** 10 November 2020; **Accepted:** 7 December 2020

Published online 20 January 2021 in Wiley Online Library (wileyonlinelibrary.com). DOI: 10.1002/mds.28489

$$\text{cUHDRS} = \left[\left(\frac{\text{TFC}-10.4}{1.9}\right) - \left(\frac{\text{TMS}-29.7}{14.9}\right) + \left(\frac{\text{SDMT}-28.4}{11.3}\right) + \left(\frac{\text{SWR}-66.1}{20.1}\right)\right] + 10$$

brain change. Histological studies have shown that neurodegeneration in HD is not uniform, following a topographically specific distribution where caudal and dorsal basal ganglia are first affected, extending then to more widespread brain areas.[11] Magnetic resonance imaging (MRI) studies have similarly demonstrated gradual atrophy and microstructural disorganization as disease progresses.[12-16] The impact of HTT lowering therapies is heterogeneous; antisense oligonucleotides (ASOs) have a more pronounced effect in the cortex, whereas RNA interference or zinc-finger proteins target the basal ganglia.[17] Therefore, there is a need for unbiased imaging methods that explore the whole brain, localizing and characterizing the relationship between brain changes and clinical markers of progression.

In the present study, we have used macro- and microstructural imaging metrics to identify specific brain areas that degenerate as clinical performance decreases in the TRACK-HD cohort of premanifest HD (pre-HD) and early-HD.[16] Here, we used voxel-based morphometry (VBM) to localize the volumetric correlates of cUHDRS and its subscales and tract-based spatial statistics (TBSS) to examine the correlations between cUHDRS and its subscales with white matter (WM) microstructural organization. We performed cross-sectional and longitudinal volumetric analyses and cross-sectional microstructural analysis and predicted that as brain volume decreased, cUHDRS performance would diminish, with congruent decreases in WM organization.

Patients and Methods

We performed our analysis on the combined group of 119 pre-HD and 119 early-HD patients from the TRACK-HD study to examine brain changes continuously across the disease course rather than imposing a potentially artificial delineation based on clinical diagnosis.[16]

We compared clinical and demographic data across groups using the 2-sample t test or ANOVA analysis for continuous variables and the χ^2 test for categoric variables.

Differences were considered significant using a probability value of 0.05.

cUHDRS is composed of 4 subscales:[6] Total Functional Capacity (TFC);[4] Total Motor Score (TMS);[4] Symbol-Digit Modality Test (SDMT),[18] and Stroop Word Reading (SWR) Test.[19] Higher scores in all scales except for TMS indicate better performance. The formula for cUHDRS is given as follows:[6]

MRI Data Acquisition, Processing, and Analysis

For a detailed description of MRI acquisition, see Supplementary data.

VBM Analysis

Baseline T1 images were bias-corrected using the N3 algorithm[20] and processed with *SPM12* (https://www.fil.ion.ucl.ac.uk/spm/software/spm12/) running in MATLAB version R2012B. T1 images were segmented and warped using DARTEL,[21,22] incorporating a modulation step and smoothed at 4 mm full-width at half-maximum for the cross-sectional VBM analysis. Within-subject quantification of change was performed using fluid registration of baseline and 36-month images. For further information, see Scahill et al.[23]

For the cross-sectional analyses, positive and negative correlations between gray matter (GM) and WM volumes and the cUHDRS and subscale scores were performed using linear regression models. For the longitudinal analysis, change in clinical scales, calculated as the difference in scores between the baseline and 36-month visits, was correlated with change in GM and WM volumes over the same period using linear regression models. Age, sex, site, total intracranial volume, and disease burden score (DBS)[24] were included as covariates. All VBM results were family-wise error rate cluster-corrected at $P = 0.05$; initial cluster-forming threshold is $P = 0.001$.

Diffusion Analysis

Diffusion-weighted imaging data were acquired during the final visit only for 3 sites. Data were analyzed using whole-brain TBSS in FSL (www.fmrib.ox.ac.uk/fsl). All subjects' FA (fractional anisotropy) data were first nonlinearly registered into a common space. Next, the mean FA image was thinned to create an FA skeleton that represented the center of all fiber bundles common to all subjects. Each participant's data were then warped onto the skeleton to perform voxelwise statistics. The same process was repeated for mean diffusivity (MD), axial diffusivity (AD), and radial diffusivity (RD) using the FA skeleton.[25]

Positive and negative correlations between all diffusivity metrics and cUHDRS and subscale scores were performed using nonparametric permutation testing

(n = 500),[26] the standard approach for TBSS analysis.[27] Only cross-sectional TBSS analyses were performed because longitudinal data were not available. Age, sex, site, and DBS were included as covariates. All TBSS results were cluster-corrected using threshold-free cluster enhancement ($P < 0.05$).[28]

Results

VBM Cross-Sectional Analyses

Imaging data from 238 participants were available. Four participants were excluded due to incomplete clinical information or failed quality control (QC). For demographic information, see Figure S1 and Table S1.

Decreased performance in the cUHDRS correlated with smaller GM volume in the basal ganglia and parietal, occipital, and insular cortices (Fig. 1). Similarly, SDMT showed a widespread positive correlation with GM volume, whereas SWR and TFC were positively associated with GM volume in the basal ganglia. Increased motor symptoms showed extensive correlations with decreased GM volume (Fig. 1).

cUHDRS also correlated positively with volume in WM surrounding the basal ganglia, occipital lobe, and centrum semiovale (Fig. 1). Higher SDMT scores were also positively associated with larger right frontal and occipital WM volume, whereas SWR and TFC showed a positive relationship with occipital WM only. TMS correlated with reduced temporal, occipital, and right frontal WM volume (Fig. S3).

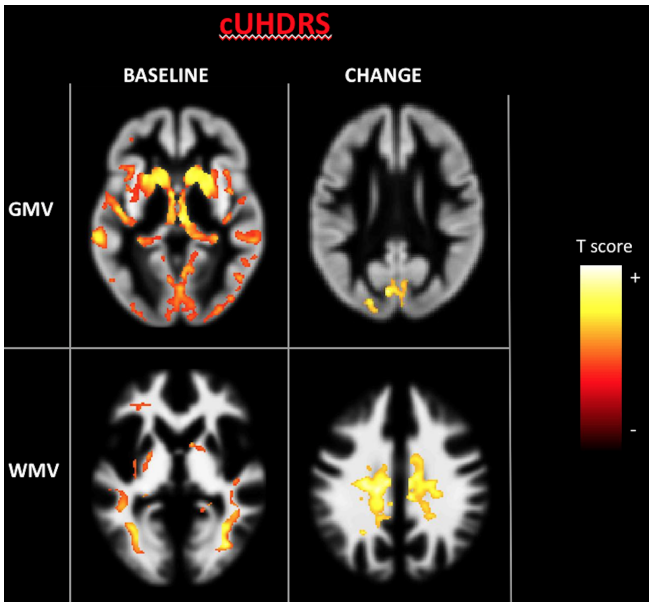

FIG. 1. Cross-sectional and longitudinal correlations between cUHDRS and brain volumes. Statistically significant correlations between baseline gray matter volume, baseline white matter volume, longitudinal change in gray matter volume, and longitudinal change in white matter volume with the cUHDRS using VBM. Baseline correlations are in the positive direction, implying that higher scores are associated with larger baseline volumes. Correlations between change in brain volume and change in cUHDRS are in the negative directions, meaning that larger decreases in brain volume would be associated with larger decreases in the cUHDRS. Results are projected onto a study-specific gray matter or white matter template. All analyses presented are adjusted by age, sex, study site, DBS, and TIV; thresholded at $P < 0.05$ (family-wise error [FWE] cluster-corrected). The color bar represents T scores (white: red, higher: lower). *cUHDRS, composite Unified Huntington's Disease Rating Scale; DBS, disease burden score; GMV, gray matter volume; TIV, total intracranial volume; VBM, voxel-based morphometry; WMV, white matter volume. [Color figure can be viewed at wileyonlinelibrary.com]

VBM Longitudinal Analyses

For the longitudinal analyses, a further 77 participants were excluded due to the absence of usable fluid-registered images or insufficient clinical information. For demographic information, see Figure S1 and S2.

Longitudinal decreases in GM volume correlated with decreased cUHDRS performance over time in the occipital and parietal cortices (Fig. 1) and decreased SDMT performance in the caudate and occipital cortex. The change in TFC was also negatively correlated with the change in GM volume in sensorimotor, prefrontal, and parietal cortices (Fig. S4).

Decreases in longitudinal WM volumes correlated with decreased scores in cUHDRS in the centrum semiovale (Fig. 1) and also with decreased performance over time in SDMT in the thalamus and midbrain. Decreases in TFC showed a widespread correlation with WM atrophy in centrum semiovale, periventricular WM, and optic radiations (Fig. S4).

There were no significant associations between the change in SWR or TMS and change in brain volumes.

DTI Cross-Sectional Analyses

Diffusion data were available for 103 participants. Of those, 21 participants were excluded due to incomplete clinical information or failed QC. For demographic information, see Figure S5 and Table S1.

cUHDRS showed associations with all 4 diffusion metrics in the corpus callosum, external capsule, temporal lobes, and subcortical WM. Higher scores in the composite were associated with increased FA and decreased AD, MD, and RD (Fig. 2). There was also widespread positive correlation between FA and SDMT. Increased motor symptoms correlated with lower values in FA, mainly in the corpus callosum and left corona radiata. Similarly, there were widespread negative correlations between MD, AD, RD, and SDMT, with congruent positive correlations between motor symptoms and all 3 diffusivity metrics (Figs. S6 and S7).

SWR and TFC did not show significant correlations with any diffusion metrics.

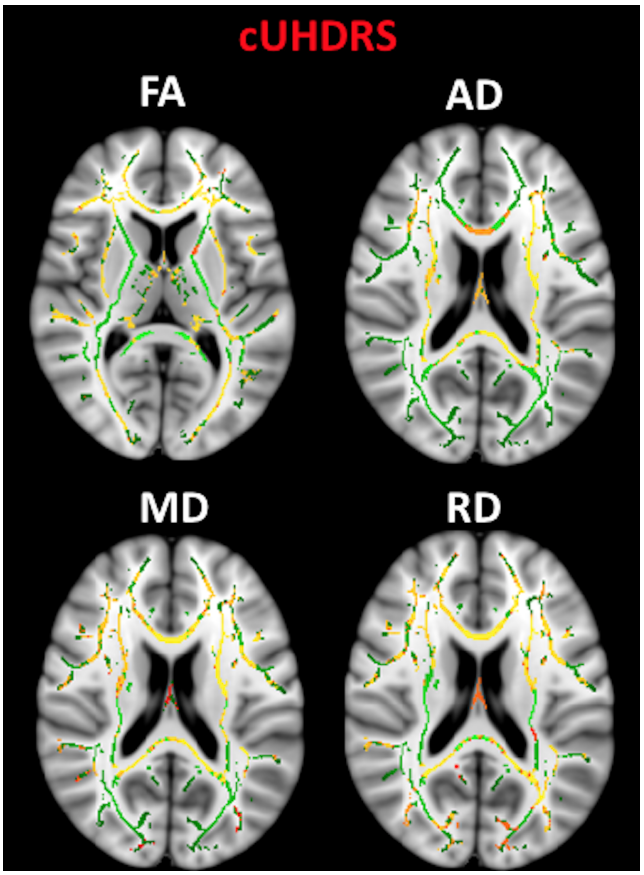

FIG. 2. Cross-sectional TBSS analysis between baseline DTI metrics and baseline cUHDRS. Correlations shown are in the negative direction except for FA where higher values mean higher coherence of white matter. Results are shown on the FA skeleton (green), overlaid on the MNI standard brain template. All analyses presented are adjusted by age, sex, study site, and DBS; thresholded at $P < 0.05$ (TFCE cluster-corrected). The colors represent *P*-values (yellow: red, higher: lower). *AD, axial diffusivity; cUHDRS, composite Unified Huntington's Disease Rating Scale; DBS, disease burden score; FA, fractional anisotropy; MD, mean diffusivity; RD, radial diffusivity; TBSS, tract-based spatial statistics; TFCE, threshold-free cluster enhancement. [Color figure can be viewed at wileyonlinelibrary.com]

Discussion

This study investigated the neural correlates of the cUHDRS, a multifaceted HD clinical measure composite, within a large pre-HD and early-HD cohort. Using unbiased whole-brain approaches, we have demonstrated that baseline brain volumes and WM organization are associated with better performance as indexed by the cUHDRS. In addition, the change in the composite is associated with longitudinal macroscopic brain changes, suggesting that an improvement in atrophy rates in the occipital cortex and centrum semiovale may mediate clinical change in the cUHDRS possibly linked to a higher longitudinal SNR compared with its subscales.

The cUHDRS composite scale has already been shown to have both excellent clinicometric properties that were above its individual constituent scales in terms of sensitivity to disease stage and association with global imaging metrics. Schobel et al performed global correlations between brain volumes using a single numeric measure for each participant (ie, total GM/caudate volume).[6] Here, we build on this approach using both volumetric and anatomical connectivity to characterize localized structural change showing that the cUHDRS is associated with imaging biomarkers in specific brain regions only.

The composite is associated with baseline GM and WM volumes in the basal ganglia and subcortical WM. In addition, longitudinal changes in the cUHDRS and atrophy track together over a clinical trial period in the centrum semiovale and occipital cortex. In line with these findings, extensive changes in subcortical WM volume, including the centrum semiovale and occipital cortical atrophy, are well known to be present in the disease,[16,29,30] being possibly related to the decreased performance in scales measuring visuospatial and visuomotor functions.

Microstructural disorganization has also been reported in pathological and previous imaging studies.[15,31-33] In agreement with these observations, the cUHDRS was linked to the integrity of the deep WM microstructure. Although further studies are required to investigate longitudinal change in diffusion metrics and their relationship with the composite, our results denote that the cUHDRS is associated with baseline imaging at both macro- and microstructural levels.

Our cross-sectional and longitudinal VBM analyses showed that the brain regions that correlated with baseline scores in the composite were different from those correlating with change in the cUHDRS. This difference may be due to *change* in clinical scores being considerably lower than that of absolute scores at baseline (Tables S1 and S2) but may also indicate that change in the brain regions over time does not necessarily reflect current disease status.

Importantly, the results of the composite are consistent across different analyses. Of the subscales, SDMT showed extensive correlations; these did not always overlap with that of the composite in terms of area, likely because the cUHDRS comprises multiple scales. TMS was associated only with cross-sectional measures, whereas TFC correlated exclusively with longitudinal changes. These results indicate that the performance of most subscales varied according to the type of analyses performed; the composite, however, showed significant results independently. The multidimensional nature of the cUHDRS together with its clinicometric properties and significant correlations with imaging biomarkers shows that the composite is most suitable for use in clinical trials.

Although our results add value to the biological significance of the cUHDRS, they require confirmation in the context of clinical trials. ASO-mediated mutant huntingtin lowering, for example, is not uniform across the brain, being more marked in the cortex and

superficial WM than in the basal ganglia,[34] both areas that correlate with cUHDRS scores in our sample. If replicated, these findings could improve the understanding of the mechanisms mediating a hypothetical benefit of the ASO in clinical function.

In terms of limitations, the number of participants differed between the cross-sectional VBM, TBSS, and longitudinal VBM studies. However, there were no significant differences in terms of DBS, age, or sex between cohorts (Table S2), and we adjusted for all demographic factors in our analyses. In addition, TBSS may be subject to misregistration and noise effects that can impact statistical significance values.[35] VBM also has potential issues when normalizing atypical brains, and smoothing can reduce localization accuracy.[36] Nevertheless, both techniques have been proven to be reliable and reproducible in HD,[9,37] and we performed detailed QC to reduce any effects of registration errors. Finally, it should be emphasized that associations between two variables require further assessments to establish a causal relationship.[38]

Conclusion

We have showed that the cUHDRS is extensively correlated with change in both brain volume cross-sectionally and longitudinally and baseline WM microstructure above its individual components. Our results provide evidence that the anatomical underpinnings of cUHDRS in the human brain are in line with disease pathology and that the composite tracks macro- and microscopic brain changes, supporting the biological relevance of the scale and shedding light on the future interpretation of the clinical trials using the cUHDRS to evaluate disease-modifying therapies in HD. ■

Acknowledgments: We thank the patients and their families.

References

1. Rodrigues FB, Abreu D, Damàsio J, et al. Survival, mortality, causes and places of death in a European Huntington's disease prospective cohort. Mov Disord Clin Pract 2017;4:737–742.
2. Mestre TA, Bachoud-Lévi A-C, Marinus J, et al. Rating scales for cognition in Huntington's disease: critique and recommendations. Mov Disord 2018;33:187–195.
3. Mestre TA, Forjaz MJ, Mahlknecht P, et al. Rating scales for motor symptoms and signs in Huntington's disease: critique and recommendations. Mov Disord Clin Pract 2018;5:111–117.
4. Huntington Study Group. Unified Huntington's disease rating scale: reliability and consistency. Mov Disord 1996;11:136–142.
5. Winder JY, Roos RAC, Burgunder J-M, et al. Interrater reliability of the unified Huntington's disease rating scale-Total motor score certification. Mov Disord Clin Pract 2018;5:290–295.
6. Schobel SA, Palermo G, Auinger P, et al. Motor, cognitive, and functional declines contribute to a single progressive factor in early HD. Neurology 2017;89:2495–2502.
7. Aylward EH, Harrington DL, Mills JA, et al. Regional atrophy associated with cognitive and motor function in prodromal Huntington disease. J Huntingtons Dis 2013;2:477–489.
8. Della Nave R, Ginestroni A, Tessa C, et al. Regional distribution and clinical correlates of white matter structural damage in Huntington disease: a tract-based spatial statistics study. Am J Neuroradiol 2010;31:1675–1681.
9. Poudel GR, Stout JC, Domínguez DJF, et al. White matter connectivity reflects clinical and cognitive status in Huntington's disease. Neurobiol Dis 2014;65:180–187.
10. Hoffman La Roche. A study to evaluate the efficacy and safety of intrathecally administered RO7234292 (RG6042) in patients with manifest Huntington's Disease. 2019. Accessed 19 Apr 2019. https://clinicaltrials.gov/ct2/show/study/NCT03761849?term=RO7234292&rank=3&show_locs=Y
11. Vonsattel JPG, Keller C, Cortes Ramirez EP. Huntington's disease - neuropathology. Hand Clin Neurol 2011;100:83–100.
12. Tabrizi SJ, Scahill RI, Durr A, et al. Biological and clinical changes in premanifest and early stage Huntington's disease in the TRACK-HD study: the 12-month longitudinal analysis. Lancet Neurol 2011;10:31–42.
13. Tabrizi SJ, Reilmann R, Roos RAC, et al. Potential endpoints for clinical trials in premanifest and early Huntington's disease in the TRACK-HD study: analysis of 24-month observational data. Lancet Neurol 2012;11:42–53.
14. Tabrizi SJ, Scahill RI, Owen G, et al. Predictors of phenotypic progression and disease onset in premanifest and early-stage Huntington's disease in the TRACK-HD study: analysis of 36-month observational data. Lancet Neurol 2013;12:637–649.
15. McColgan P, Seunarine KK, Razi A, et al. Selective vulnerability of Rich Club brain regions is an organizational principle of structural connectivity loss in Huntington's disease. Brain 2015;138:3327–3344.
16. Tabrizi SJ, Langbehn DR, Leavitt BR, et al. Biological and clinical manifestations of Huntington's disease in the longitudinal TRACK-HD study: cross-sectional analysis of baseline data. Lancet Neurol 2009;8:791–801.
17. Wild EJ, Tabrizi SJ. Therapies targeting DNA and RNA in Huntington's disease. Lancet Neurol 2017;16:837–847.
18. Parmenter BA, Weinstock-Guttman B, Garg N, Munschauer F, Benedict RHB. Screening for cognitive impairment in multiple sclerosis using the symbol digit modalities test. Mult Scler J 2007;13:52–57.
19. Stroop JR. Studies of interference in serial verbal reactions. J Exp Psychol 1935;18:643–662.
20. Sled JG, Zijdenbos AP, Evans AC. A nonparametric method for automatic correction of intensity nonuniformity in MRI data. IEEE Trans Med Imaging 1998;17:87–97.
21. Ashburner J. A fast diffeomorphic image registration algorithm. Neuroimage 2007;38:95–113.
22. Good CD, Johnsrude IS, Ashburner J, Henson RN, Friston KJ, Frackowiak RS. A voxel-based morphometric study of ageing in 465 normal adult human brains. Neuroimage 2001;14:21–36.
23. Scahill RI, Schott JM, Stevens JM, Rossor MN, Fox NC. Mapping the evolution of regional atrophy in Alzheimer's disease: unbiased analysis of fluid-registered serial MRI. Proc Natl Acad Sci U S A 2002;99:4703–4707.
24. Penney JB, Vonsattel JP, MacDonald ME, Gusella JF, Myers RH. CAG repeat number governs the development rate of pathology in Huntington's disease. Ann Neurol 1997;41:689–692.
25. Smith SM, Jenkinson M, Johansen-Berg H, et al. Tract-based spatial statistics: Voxelwise analysis of multi-subject diffusion data. Neuroimage 2006;31:1487–1505.
26. Winkler AM, Ridgway GR, Webster MA, Smith SM, Nichols TE. Permutation inference for the general linear model. Neuroimage 2014;92:381–397.
27. Nichols TE, Holmes AP. Nonparametric permutation tests for functional neuroimaging: a primer with examples. Hum Brain Mapp 2002;15:1–25. https://doi.org/10.1002/hbm.1058
28. Smith SM, Nichols TE. Threshold-free cluster enhancement: addressing problems of smoothing, threshold dependence and localisation in cluster inference. Neuroimage 2009;44:83–98.
29. Johnson EB, Rees EM, Labuschagne I, et al. The impact of occipital lobe cortical thickness on cognitive task performance: an investigation in Huntington's disease. Neuropsychologia 2015;79:138–146.
30. Rosas HD, Liu AK, Hersch S, et al. Regional and progressive thinning of the cortical ribbon in Huntington's disease. Neurology 2002;58:695–701.

31. Scahill RI, Hobbs NZ, Say MJ, et al. Clinical impairment in premanifest and early Huntington's disease is associated with regionally specific atrophy. Hum Brain Mapp 2013;34:519–529.

32. van den Bogaard SJA, Johnson H, Scahill RI, et al. Early atrophy of pallidum and accumbens nucleus in Huntington's disease. J Neurol 2010; 258:412–420.

33. Vonsattel JP, Myers RH, Stevens TJ, Ferrante RJ, Bird ED, Richardson EP Jr. Neuropathological classification of Huntington's disease. J Neuropathol Exp Neurol 1985;44:559–577.

34. Kordasiewicz HB, Stanek LM, Wancewicz EV, et al. Sustained therapeutic reversal of Huntington's disease by transient repression of huntingtin synthesis. Neuron 2012;74:1031–1044.

35. Bach M, Laun FB, Leemans A, et al. Methodological considerations on tract-based spatial statistics (TBSS). Neuroimage 2014;100:358–369.

36. Mechelli A, Price CJ, Friston KJ, Ashburner J. Voxel-based morphometry applications of the human brain: methods and applications. Curr Med Imaging Rev 2005;1:105–113.

37. Henley SMD, Ridgway GR, Scahill RI, et al. Pitfalls in the use of voxel-based morphometry as a biomarker: examples from Huntington disease. Am J Neuroradiol 2010;31:711–719.

38. Scahill RI, Andre R, Tabrizi SJ, Aylward EH. Structural imaging in premanifest and manifest Huntington disease. Handb Clin Neurol 2017;144:247–261.

Supporting Data

Additional Supporting Information may be found in the online version of this article at the publisher's web-site.

Gabapentin Relieves Vertigo of Periodic Vestibulocerebellar Ataxia: 3 Cases and Possible Mechanism

J. Thaddeus Coin, PhD, MD,[1*] and Jeffery M. Vance, PhD, MD[2]

[1]*Wilmington, North Carolina, USA* [2]*Dr. John T. Macdonald Foundation Department of Human Genetics, Department of Neurology, Hussman Institute for Human Genomics, Miller School of Medicine, University of Miami, Miami, Florida, USA*

*__Correspondence to:__ Dr. J. Thaddeus Coin, 2515 Delaney Avenue, Wilmington, NC 28403, USA; E-mail: jtcoinneurology@gmail.com

Relevant conflicts of interest/financial disclosures: Nothing to report.

Funding agencies: There is no sponsorship or funding for this study.

"Full financial disclosures and author roles may be found in the online version of this article."

Received: 8 October 2020; **Revised:** 25 November 2020; **Accepted:** 21 December 2020

Published online 16 January 2021 in Wiley Online Library (wileyonlinelibrary.com). DOI: 10.1002/mds.28491

ABSTRACT: Objective: The aim of this study was to report relief of optokinetic-triggered vertigo (OKTV) with low-dose gabapentin in three patients with periodic vestibulocerebellar ataxia [episodic ataxia type 4 (EA4); OMIM 606552].

Methods: Clinical observations and analysis of video-recorded eye movements were used before and after gabapentin.

Results: Gabapentin relieved vertigo of all three treated patients with EA4, particularly during activities that typically would induce vertiginous symptoms. Two patients reported 8–12 hours of sustained relief after the first 100 mg dose. One has benefited from 100–200 mg TID for 7 years. Video analysis of nystagmus revealed improved target tracking on smooth pursuit and a steadier gaze hold.

Conclusions: Gabapentin effectively relieved the optokinetic-triggered vertigo in our patients with EA4. Mechanisms are postulated in terms of known tight gabapentin binding to the Purkinje cell voltage-gated calcium channel. The observations may offer insight into this rare disease's neuropathology. © 2021 International Parkinson and Movement Disorder Society

Key Words: periodic vestibulocerebellar ataxia; episodic ataxia; autosomal dominant ataxia; gabapentin; optokinetic vertigo

Periodic vestibulocerebellar ataxia [episodic ataxia type 4 (EA4[1]); OMIM 606552[2]] is an adult-onset, autosomal dominant (AD) cerebellar ataxia characterized by prominent eye coordination symptoms, including optokinetic-triggered vertigo (OKTV) followed universally by progressive cerebellar ataxia. The first known affected family was reported in 1963 by Farmer and Mustian.[3] This and subsequently described families likely belong to a single kindred, distinct from other genetically defined AD ataxias, originating from the same rural North Carolina community.[4–7] The OKTV has been correlated with examination findings: gaze-induced nystagmus and vestibulo-ocular reflex nonsuppression demonstrated by the "clothes hanger hat" test.[6] The patient sits motionless in a slowly spun swivel chair, eyes fixed on a target suspended by the hat. Easily observed nystagmus is triggered by the moving scene. The deficits localize to the cerebellar flocculus,[6] supported by postmortem examination.[8]

OKTV will often occur in affected EA4 individuals while grocery shopping. Due to patients' attempts to steady themselves with the grocery cart, Farris et al.[5] informally referred to the symptom complex as the "shopping cart syndrome" (Bradley K. Farris, personal communication). Patients examined by Small et al.[6] described the same. When attempting to fix on shelved